Loss-of-Control: Perspectives on Flight Dynamics and Control of Impaired Aircraft

Harry G. Kwatny [*], Jean-Etienne T. Dongmo [†], Robert C. Allen [‡] and Bor-Chin Chang [§]

Drexel University, 3141, Chestnut Street, Philadelphia, PA, 19104.

Gaurav Bajpai [¶]

Techno-Sciences, Inc., 11750 Beltsville Road, Beltsville, MD, 20705.

Loss-of-Control **(LOC) is a major factor in fatal aircraft accidents. Although definitions of LOC remain vague in analytical terms, it is generally associated with a significantly diminished capability of the pilot to control the aircraft. In previous work we considered how the ability to regulate an aircraft deteriorates around stall points. In this paper we examine how damage to control effectors impacts the capability to keep the aircraft within an acceptable envelope and to maneuver within it. We show that even when a sufficient set of steady motions exist, the ability to regulate around them or transition between them can be difficult and nonintuitive, particularly for impaired aircraft.**

Nomenclature

x	State vector
y	Measurements
z	Regulated variables
μ	System parameters
u	Control inputs
α	Angle of attack, deg
β	Side slip angle, deg
V	Velocity, ft/s
X	x inertial coordinate, ft
Y	y inertial coordinate, ft
Z	z inertial coordinate, ft
p	x body-axis angular velocity component, deg/s
q	y body-axis angular velocity component, deg/s
r	z body-axis angular velocity component, deg/s
u	x body-axis translational velocity component, ft/s
v	y body-axis translational velocity component, ft/s
w	z body-axis translational velocity component, ft/s
ϕ	Euler roll angle, deg
θ	Euler pitch angle, deg
ψ	Euler yaw angle, deg
Ψ	Heading, deg
γ	Flight path angle, deg
A	System matrix of a linear system
B	Control matrix of a linear system

[*]S. Herbert Raynes Professor, AIAA Member

[†]Graduate Student, AIAA Student Member

[‡]Graduate Student, AIAA Student Members

[§]Professor, AIAA Member

[¶]Director, Dynamics and Control, AIAA Member

C	Output matrix of a linear system
T	Thrust, lbf
δ_e	elevator input, deg
δ_a	Aileron input, deg
δ_r	Rudder input, deg
$\mathcal{C}$	envelope
$\mathcal{S}$	safe set
$\mathcal{U}$	control constraint set
$\mathcal{T}$	trim manifold

I. Introduction

There is ample evidence indicating that *Loss-of-Control* (LOC) is a major factor in fatal aircraft accidents (for example, [1–3]). While definitions of LOC remain vague in analytical terms,[4,5] it is generally associated with flight outside the normal flight envelope, nonlinear behaviors and, most importantly, with an inability of the pilot to control the aircraft. In previous work[6,7] we considered how controllability and the ability to regulate an aircraft deteriorate around static bifurcation (stall) points. It was shown that the correct control strategies in neighborhoods of these points could change abruptly, contributing to confusion and with the consequent possibility of inappropriate pilot inputs. In [7], we also illustrated how control bounds can effect the ability of a pilot to keep the aircraft within its admissible flight envelope which ordinarily excludes such bifurcation points.

In this paper we further examine the issues associated with keeping the aircraft, unimpaired or impaired, within its prescribed envelope and the extent to which it can maneuver within it. Loosely stated, there are four basic questions:

1. Is it possible to keep the aircraft within its flight envelope?
2. Can the aircraft maneuver satisfactorily within the envelope?
3. How can departure from it be prevented?
4. How can the aircraft state be restored to the envelope in the event that it departs from it?

Here we focus on the first two questions. The first question can be addressed in terms of the concept of a *safe set* or *viable set*.[8,9] Safe set theory could be used as a basis for envelope protection and prevention of some forms of LOC, but this idea has not been fully developed. The idea of a safe set derives from a decades old control problem in which the plant controls are restricted to a bounded set $\mathcal{U}$ and it is desired to keep the system state within a convex, not necessarily bounded, subset $\mathcal{C}$ of the state space. Feuer and Heyman[10] studied the question: under what conditions does there exist for each initial state in $\mathcal{C}$ an admissible control producing a trajectory that remains in $\mathcal{C}$ for all $t > 0$? When $\mathcal{C}$ does not have this property we try to identify the safe set, $\mathcal{S}$, that is, the largest subset of $\mathcal{C}$ that does. Clearly, if we wish the aircraft to remain in $\mathcal{C}$, we must insure that it remains in $\mathcal{S}$.

We would also like to know how the aircraft can maneuver within $\mathcal{S}$. Controlled flight requires the existence of a suitable set of steady motions and the ability to smoothly transition between them. This means that we need to understand the equilibrium point structure within $\mathcal{S}$ and we need to identify any impediments to regulating around them or steering from one to another. These questions are examined in this paper.

Ordinarily, if a an aircraft is impaired we expect that the safe set will shrink. We will show that the equilibrium point structure within the reduced safe set changes as well and the ability to maneuver is significantly diminished. Furthermore, control strategies required to execute transition maneuvers and to regulate around steady motions may be complex and non-intuitive. We suggest this as another mechanism of LOC. Examples are based on NASA's Generic Transport Model (GTM).[11]

The organization of the paper is as follows. In Section II we discuss the GTM and the mathematical models we use. As a simple illustrative example, we will use the phugoid dynamics of the GTM. This model is also described. In Section III we discuss the safe set, some of its properties, and provide examples for unimpaired and impaired aircraft. In Section IV we consider maneuverability and illustrate the effect of actuator impairment. Finally, Section V contains some concluding remarks.

II. Dynamics of the GTM

In the subsequent discussion we will provide examples based on NASA's Generic Transport Model (GTM). Data obtained from NASA have been used to develop symbolic and simulation models. Nonlinear symbolic models are used to perform bifurcation analysis and nonlinear control analysis and design. Linear Parameter Varying (LPV) models are derived from the nonlinear symbolic model and have been used to study the variation in the structure of the linear control system properties around bifurcation points. Simulation models are also automatically assembled from the symbolic model in the form of optimized C-code that compiles as a MEX file for use as an S-function in Simulink. The GTM model is described in Section A.

In the following discussion we will use a simple recurring example to illustrate several important concepts. The example is based on the phugoid dynamics of the GTM. Besides being a useful example in its own right, it has the distinct advantage for us in that it has a two dimensional state space allowing us to provide simple graphical illustrations of complex general principles. In Section B we describe the model and illustrate some basic steady motions predicted by the phugoid model.

A. The Generic Transport Model

The six degrees of freedom aircraft model has 12 or 13 states depending on whether we use Euler angles or quaternions. In the Euler angle case the model is generated in the form of Poincaré's equations,[12]

$$\dot{\mathbf{q}} = V(\mathbf{q})\,\mathbf{p} \tag{1}$$

$$M(\mathbf{q},\mu)\,\dot{\mathbf{p}} + C(\mathbf{q},\mu)\,\mathbf{p} + F(\mathbf{p},\mathbf{q},\mu,\mathbf{u}) = 0 \tag{2}$$

where $\mathbf{q} = (\phi,\theta,\psi,X,Y,Z)^T$ is the generalized coordinate vector and $\mathbf{p} = (p,q,r,u,v,w)^T$ is the (quasi-) velocity vector. We can combine the kinematics (1) and dynamics (2) to obtain the state equations

$$\dot{x} = f(x,u,\mu) \tag{3}$$

where $\mu \in R^k$ is an explicitly identified vector of distinguished aircraft parameters such as mass or center of mass location (or even set points for regulated variables), $x \in R^n$ is the state vector, and $u \in R^m$ is the control vector. In the Euler angle case, $n = 13$ and the state is given by $x = [\phi,\theta,\psi,X,Y,Z,p,q,r,u,v,w]^T$. There are 4 control inputs, given by $u = [T,\delta_e,\delta_a,\delta_r]^T$. The controls are limited as follows: thrust $0 \le T \le 40$ lbf, elevator $-40^\circ \le \delta_e \le 20^\circ$, aileron $-20^\circ \le \delta_e \le 20^\circ$, and rudder $-30^\circ \le \delta_e \le 30^\circ$. Velocity is in ft/s.

Aerodynamic models were obtained from NASA. They are based on data obtained with a 5.5 % scale model in the NASA Langley 14 ft × 22 ft wind tunnel as described in.[13] Aerodynamic force and moment coefficients are generated using a multivariate orthogonal function method as described in.[14,15] In the original NASA model several regions of angle of attack were used to capture severe nonlinearity. These models were blended using Gaussian weighting. For simplicity we use only one of the models for the analysis herein.

B. The Phugoid Model

The longitudinal dynamics of a rigid aircraft can be written in path coordinates:

$$\begin{aligned}
&\dot{\theta} = q \\
&\dot{x} = V\cos\gamma \\
&\dot{z} = V\sin\gamma \\
&\dot{V} = \tfrac{1}{m}\left(T\cos\alpha - \tfrac{1}{2}\rho V^2 S C_D(\alpha,\delta_e,q) - mg\sin\gamma\right) \\
&\dot{\gamma} = \tfrac{1}{mV}\left(T\sin\alpha + \tfrac{1}{2}\rho V^2 S C_L(\alpha,\delta_e,q) - mg\cos\gamma\right) \\
&\dot{q} = \tfrac{M}{I_y}, \quad M = \left(\tfrac{1}{2}\rho V^2 S\bar{c}C_m(\alpha,\delta_e,q) + \tfrac{1}{2}\rho V^2 S\bar{c}C_Z(\alpha,\delta_e,q)(x_{cgref} - x_{cg}) - mgx_{cg} + l_t T\right) \\
&\alpha = \theta - \gamma
\end{aligned} \tag{4}$$

A classic analysis problem of aeronautics was introduced by Lanchester[16] over one hundred years ago – the long period *phugoid* motion of an aircraft in longitudinal flight. The phugoid motion is a roughly constant angle of attack behavior involving an oscillatory pitching motion with out of phase variation of altitude and speed. The ability to stabilize the phugoid motion using the elevator or thrust is important. The inability to do so has been linked to a number of fatal airline accidents including Japan Airlines Flight 123 in 1985 and United Airlines Flight 232 in 1989.[17]

We will illustrate several computations by examining the controlled phugoid dynamics of the GTM. The problem is similar to one considered in [8,18] to illustrate safe set computations. The key assumption is that pitch rate rapidly approaches zero so that the the phugoid motion is characterized by $q \equiv 0$. Thus, we must have

$$M = \left(\tfrac{1}{2}\rho V^2 S\bar{c}C_m\left(\alpha,\delta_e,q\right) + \tfrac{1}{2}\rho V^2 S\bar{c}C_Z\left(\alpha,\delta_e,q\right)\left(x_{cgref}-x_{cg}\right) - mgx_{cg} + l_tT\right) = 0 \tag{5}$$

From (5) we obtain a quasi-static approximation for the angle of attack

$$\alpha = \widehat{\alpha}\left(V,T,\delta_e\right) \tag{6}$$

so that the $V-\gamma$ equations in (4) decouple from the remaining equations. Thus, we have a closed system of two differential equations that define the phugoid dynamics:

$$\begin{aligned}\dot{V} &= \tfrac{1}{m}\left(T\cos\widehat{\alpha} - \tfrac{1}{2}\rho V^2 SC_D\left(\widehat{\alpha},\delta_e,0\right) - mg\sin\gamma\right)\\ \dot{\gamma} &= \tfrac{1}{mV}\left(T\sin\widehat{\alpha} + \tfrac{1}{2}\rho V^2 SC_L\left(\widehat{\alpha},\delta_e,0\right) - mg\cos\gamma\right)\end{aligned} \tag{7}$$

The angle of attack, α can be considered as an output as given by equation (5).

We specify an operating envelope

$$\mathcal{C} = \left\{\left(V,\gamma\right)\left|90 \le V \le 240, -22 \le \gamma \le 22\right.\right\}$$

and control restraint set

$$\mathcal{U} = \left\{\left(T,\delta_e\right)\left|0 \le T \le 40, -40 \le \delta_e \le 20\right.\right\}$$

C. Steady Motion

We first examine the trim motion associated with a specified speed and flight path angle. In accordance with (7), with V and γ specified, we need to find T and δ_e such that

$$\begin{aligned}0 &= T\cos\widehat{\alpha} - \tfrac{1}{2}\rho V^2 SC_D\left(\widehat{\alpha},\delta_e,0\right) - mg\sin\gamma\\ 0 &= T\sin\widehat{\alpha} + \tfrac{1}{2}\rho V^2 SC_L\left(\widehat{\alpha},\delta_e,0\right) - mg\cos\gamma\end{aligned} \tag{8}$$

As an example suppose we wish to examine steady flight with $\gamma = 0$ and various speeds. Beginning with the trim condition: $V = 150$ fps, $\gamma = 0$ deg, $T = 4.0991$ lbf, $\delta_e = 1.725$ deg we perform a continuation analysis to obtain the results in Figure .1. The corrsponding initial value for angle of attack is $\alpha = 2.96644$ deg.

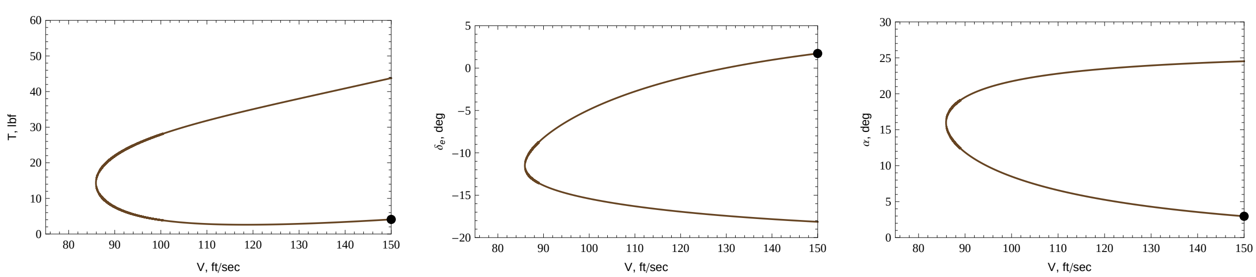

(a) Thrust (b) Elevator Position (c) Angle of Attack

Figure .1. The figure shows the trim values for thrust, elevator and angle of attack for various values of airspeed, V, and $\gamma = 0$. Note that the starting point for the continuation is identified by the black dot.

Starting at the black dot, as airspeed drops the trim points follow the lower branch of the thrust and angle of attack curves and the upper branch of the elevator curve until the bifurcation (stall) point is reached ($V = 85.9150$ fps, $T = 14.3440$ lbf, $\delta_e = -11.5059$ deg). These are the 'normal' trim points, but the alternate branch is also comprised of viable trim points so long as the thrust and elevator are within bounds. This observation can be important, as we will see below. We might refer to these as *high angle of attack* trim points.

An essential point is that the control behaviors around trim points on the two branches are considerably different so that a strategy to regulate around a point on one branch will fail if applied to one on the other branch. The theoretical basis for this is established in [6,19–21]. We will give a simple example. Consider the two trim points at 90 fps, the *normal trim point*, $V = 90$ fps, $\gamma = 0$ deg, $T = 7.58222$ lbf, $\delta_e = -8.22916$ deg and the *high angle of attack trim point*, $V = 90$ fps, $\gamma = 0$ deg, $T = 21.9189$ lbf, $\delta_e = -13.8494$ deg. The linear dynamics at each of these trim points is, first for the normal trim:

$$\frac{d}{dt}\left[\begin{array}{c}\Delta V\\ \Delta\gamma\end{array}\right] = \left[\begin{array}{cc}-0.186044 & -33.2125\\ 0.008844275 & 0.0150152\end{array}\right]\left[\begin{array}{c}\Delta V\\ \Delta\gamma\end{array}\right] + \left[\begin{array}{cc}0.449195 & 62.3033\\ 0.00416546 & -0.751226\end{array}\right]\left[\begin{array}{c}\Delta T\\ \Delta\delta_e\end{array}\right]$$

and for the high angle of attack trim:

$$\frac{d}{dt}\left[\begin{array}{c}\Delta V\\ \Delta\gamma\end{array}\right] = \left[\begin{array}{cc}-0.310011 & -33.2514\\ 0.00638713 & -0.0338864\end{array}\right]\left[\begin{array}{c}\Delta V\\ \Delta\gamma\end{array}\right] + \left[\begin{array}{cc}0.494357 & 31.5244\\ -0.00127241 & 1.22673\end{array}\right]\left[\begin{array}{c}\Delta T\\ \Delta\delta_e\end{array}\right]$$

Inspection of the control input matrix shows the reversal of the affect of the elevator, δ_e. Ay the normal trim a positive (counterclockwise) rotation of the elevator causes a reduction of the flight path angle, i.e., pitch down. On the other hand, at the high angle attack trim a positive elevator rotation causes an increase in flight path angle.

This behavior is organized by the singular zero dynamics at the bifurcation point that separates the two branches. The state equations linearized at the bifurcation point are

$$\frac{d}{dt}\left[\begin{array}{c}\Delta V\\ \Delta\gamma\end{array}\right] = \left[\begin{array}{cc}-0.27235 & -33.8550\\ 0.00791414 & -0.00286013\end{array}\right]\left[\begin{array}{c}\Delta V\\ \Delta\gamma\end{array}\right] + \left[\begin{array}{cc}0.400642 & 62.5119\\ 0.00170008 & 0.265262\end{array}\right]\left[\begin{array}{c}\Delta T\\ \Delta\delta_e\end{array}\right]$$

Inspection of the two columns of the control input matrix shows that they are dependent – the second obtained from the first by multiplication by 156.029. Thus, the controls are redundant. There is only one effective control direction. The important implication is that, from a linear perspective, both V and γ cannot be simultaneously regulated.[22] Another indication of the degeneracy of the linearized system at the bifurcation point is the degeneracy of the transfer matrix, $G(s)$, $(T, \delta_e) \to (V, \gamma)$:

$$G(s) = \frac{1}{s^2 + 0.27521s + 0.268712}\left[\begin{array}{cc}0.400642s - 0.0564101 & 62.5119s - 8.80163\\ 0.001700086 + 0.00363376 & 0.265262s + 0.566973\end{array}\right]$$

A simple computation shows that $|G(s)| \equiv 0$.

III. The Safe Set

The idea of the *safe set* was introduced in[18,23] and subsequently developed in several other papers including.[8,9]

A. Control with state and control constraints

All aircraft are required to operate within a specified flight envelope. For example, a typical unimpaired aircraft will have limitations and on load factor, attitude and speed. Indeed most aircraft employ envelope protection strategies. While there is no comprehensive theory of envelope protection, it has been addressed in the literature, for example.[23–25] An important factor is that protective control actions are themselves limited. For example, control surfaces have a restricted range of motion and are limited in the control forces that can be generated by them.

Consider a controlled dynamical system

$$\dot{x} = f(x, u), \quad x \in R^n, u \in \mathcal{U} \subset R^m \tag{9}$$

where the set $\mathcal{U}$ is closed, bounded and convex. Also, suppose the desired envelope is a convex, not necessarily bounded, subset $\mathcal{C}$ of the state space R^n. Feuer and Heyman[10] study the general control problem of interest. Specifically, under what conditions does there exist for each $x_0 \in \mathcal{C}$ a control $u(t) \subset U$ and a corresponding unique solution $x(t; x_0, u)$ that remains in $\mathcal{C}$ for all $t > 0$? While some basic results are provided in [10], the general case is unresolved. Concrete results have subsequently been obtained for special cases, particularly for linear dynamics with polyhedral constraint sets.[8,9,18,26–30] In the following paragraphs we apply some of the more recent results.[8,9,18]

Suppose that prescribed envelope $\mathcal{C}$ is defined by

$$\mathcal{C} = \{x \in R^n \,|l(x) > 0\} \tag{10}$$

where $l : R^n \to R$ is continuous. The boundary of $\mathcal{C}$ is the zero level set of l, i.e., $\partial\mathcal{C} = \{x \in R^n \,|l(x) = 0\}$.

Definition 3.1 (Controlled-Invariant Set) *A set $\mathcal{I}$ is a controlled-invariant set over a time interval $[t, T]$, if for each $x(t) \in \mathcal{I}$ there exists a control $u(\tau) \in \mathcal{U}$, $\tau \in [t, T]$ such that the solution of (9) emanating from $x(t)$, $\phi(\tau; x(t), u(\cdot))$, defined on $\tau \in [t, T]$ is entirely contained in $\mathcal{I}$.*

Definition 3.2 (Safe Set) *Given the envelope $\mathcal{C}$ as defined in (10), the safe set is defined as the largest controlled-invariant set on $[t, T]$ contained in $\mathcal{C}$, i.e.,*

$$\mathcal{S}(t, \mathcal{C}) = \{x \in R^n \,|\exists u(\tau) \subset \mathcal{U}, \forall\tau \in [t, T] : \phi(\tau; x(t), u(\cdot)) \subset \mathcal{C}\} \tag{11}$$

Several investigators have considered the computation of the safe set, the most compelling of which involve solving the Hamilton-Jacobi equation. We describe one of several variants; this one due to Lygeros.[8] The main result in [8] is the following. Suppose $V(x, t)$ is a viscosity (or, weak) solution of the terminal value problem

$$\frac{\partial V}{\partial t} + \min\left\{0, \sup_{u\in U} \frac{\partial V}{\partial x} f(x, u)\right\} = 0, \quad V(x, T) = l(x) \tag{12}$$

then

$$\mathcal{S}(t, \mathcal{C}) = \{x \in R^n \,|V(x, t) > 0\} \tag{13}$$

The function $V(x, t)$ is in fact the 'cost-to-go' associated with an optimal control problem in which the goal is to choose $u(t)$ so as to maximize the minimum value of $l(x(t))$. The function $V(x, t)$ inherits some nice properties from this fact. For instance it is bounded and uniformly continuous. Define the Hamiltonian

$$H(p, x) = \min\left\{0, \sup_{u\in U} p^T f(x, u)\right\} \tag{14}$$

so that (12) can be rewritten:

$$\frac{\partial V}{\partial t} + H\left(\frac{\partial V}{\partial x}, x\right) = 0, \quad V(x, T) = l(x) \tag{15}$$

$V(x, t)$ is the unique, bounded and uniformly continuous solution of (12) or (15). Notice that the control obtained in computing the Hamiltonian (14) insures that when applied to each state along any trajectory initially inside of $\mathcal{S}$ the resulting trajectory will remain in $\mathcal{S}$. It follows that this control should be applied for states on its boundary to insure that the trajectory does not leave $\mathcal{S}$.

The envelope defined by (10) can be generalized to an envelope with piecewise continuous boundary. For example, suppose the envelope is defined by

$$\mathcal{C} = \{x \in R^n \,|l_i(x) > 0, i = 1, \ldots, K\} \tag{16}$$

Where each of the $l_i(x)$ are continuous functions. Then we need to solve K problems with

$$\mathcal{C}_j = \{x \in R^n \,|l_j(x) > 0\}, \quad j = 1, \ldots, K$$

to obtain the largest control invariant set in each $\mathcal{C}_j$ and then take their intersection. There are many physical problems in which the tracking of moving boundaries separating to regions of space are important. So it is not surprising that the numerical computation of propagating surfaces is a mature field. The most powerful methods exploit the connection with the Hamilton-Jacobi equation and associated conservation laws; see the survey [31].

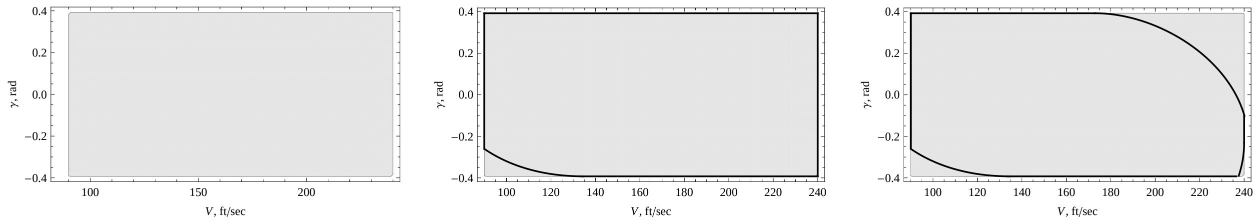

(a) Unimpaired (b) Restricted Elevator (c) Jammed Elevator

Figure .2. Safe set with various levels of elevator impairment. The figure on the left shows the safe set for the unimpaired aircraft in which case the elevator position ranges from -40 deg (-0.698 rad) to +20 deg (0.349 rad). It is the entire envelope. In the center figure, the elevator motion is restricted in the positive direction to + 3 deg. On the right is the safe set for the aircraft with elevator jammed at 3 deg. The safe set is the subset of the flight envelope bounded by the black curve.

B. Example: GTM Phugoid Motion

Figure .2 shows the safe set, $\mathcal{S}$ for unimpaired and impaired aircraft. As expected, the safe set shrinks when the aircraft is impaired. The points in $\mathcal{C}\backslash\mathcal{S}$ produce trajectories that exit the envelope. With limited control authority the safe set is reduced in lower left quadrant of (b,c) because at slower speeds, even with the application of both maximum thrust and elevator deflection, it is not possible to generate enough lift to prevent the aircraft from descending along an unacceptably low flight path angle and leaving the prescribed envelope $\mathcal{C}$. In the case where the elevator is jammed, the safe set is reduced in the upper right quadrant (c) where the higher speeds cause excessive lift to be generated forcing the aircraft to ascend along a flight path angle which exceeds the upper bound of $\mathcal{C}$.

IV. Maneuverability

Diminished maneuverability is a central aspect of LOC - whether due to impairment of the aircraft or its entry into an unfavorable flight regime. Maneuverability performance is usually assessed by evaluating an aircraft's capability to perform certain basic tasks under a variety of conditions. Such tasks – including wings level climb and descent, coordinated turns, pull-ups and push-downs – correspond to *steady-state* or *equilibrium* motions in an appropriate mathematical setting. The vehicle must be able to transition between these steady motions.

In earlier work[6] we introduced an approach to investigating steady motions of aircraft by examining the equilibrium point structure of a regulator problem associated with the desired motion. We used a continuation method to identify bifurcation surfaces in multi-parameter problems and linked bifurcation points to structural instability of the zero dynamics. The limits imposed on the ability of a vehicle to perform a maneuver where thereby associated with both the absence of appropriate equilibria for certain parameter values and also with the difficulty to regulate the vehicle when operating near the bifurcation sets. These ideas were further developed and applied in several papers including [7, 32, 33]. A somewhat similar approach was recently given by Goman et al,[34] referred to therein as a *constrained trim formulation*. The stability of each equilibrium point is evaluated but no connections are made to control system properties as advocated in [6].

A. Basic Steady Maneuvers of Rigid Aircraft

For commercial aircraft the most basic and important steady motion are:

1. straight, level, climbing and descending flight,
2. coordinated turns, level, climbing and descending

In [7] we used a continuation method to examine these motions specifically for the GTM. We studied the limits imposed on these motions by stall bifurcation points and examined the control system behavior around these points. Using the results of [6] we argued that regulated flight near stall is difficult because of the structurally unstable zero dynamics.

Of course, not all points identified in a continuation computation are feasible trim conditions. Equilibria with control values outside of the control restraint set need to be excluded. This obvious fact has significant implications as we will see below.

The idea of aircraft trim is so broadly entrenched that one would assume it requires no further discussion. However, there are subtleties that we need to explore. A general formulation is as follows. Assume the aircraft is described by the state equations in the form of (1) and (2), or (3).

Definition 4.3 (Steady Motion) *A* steady motion *is one for which all 6 velocities are constant, i.e., $\dot{u}=0, \dot{v}=0, \dot{w}=0$, (equivalently, $\dot{V}=0,\ \dot{\alpha}=0, \dot{\beta}=0$) and $\dot{p}=0, \dot{q}=0,\ \dot{r}=0$. From (2)*

$$F\left(0,\mathbf{q},\mu,\mathbf{u}\right)=0 \tag{17}$$

The steady motion requirement, (17), provides six equations to which we add a set of $n+m-6$ *trim* equations:

$$0=h\left(x,u,\mu\right) \tag{18}$$

Equations (17) and (18) form a set of $n+m$ equations in $n+m+k$ variables. Ordinarily we fix the k parameters, μ and solve for the remaining $n+m$ variables – the state x and the control u.

Definition 4.4 (Trim Point) *Given the steady motion equation (17), the trim condition (18), an envelope $\mathcal{C}$ and a control restraint set $\mathcal{U}$, a* viable trim point *or simply a* trim point*, with respect to the fixed parameter μ is a pair (x,u) that satisfies (17) and (18) and also $x\in\mathcal{C}$, $u\in\mathcal{U}$. The set of viable trim points is called the* trim set*, $\mathcal{T}$.*

The important point is that for a prescribed trim condition (18) there are often multiple viable trim points. The general study of the trim point structure as a function of the parameters is a problem of static bifurcation analysis.[6,7,33,35,36] When $k=1$ this can be carried out using a continuation method. Let us consider two examples of the trim condition for the six degree of freedom model described in Section II. In this case we have four controls. First consider straight wings-level flight:

1. speed, $V=V^*$
2. constant roll, pitch and heading, $\dot{\phi}=0, \dot{\theta}=0,\ \dot{\psi}=0$
3. roll angle, $\phi=0$
4. flight path angle, $\sin\gamma^*+\cos\theta\left(\cos\beta\cos\phi\sin\alpha+\sin\beta\sin\phi\right)-\cos\alpha\cos\beta\sin\theta=0$

Now, consider a coordinated turn. In this case the aircraft rotates at constant angular velocity, ω^* about the inertial z-axis. Thus the attitude of the aircraft varies periodically with time.

1. speed, $V=V^*$
2. coordinate turn condition, $pV\cos\beta\sin\alpha-rV\cos\beta\cos\alpha+g\cos\theta\sin\phi=0$
3. angular velocity, $p=-\omega^*\sin\theta, q=\omega^*\cos\theta\sin\phi, r=\omega^*\cos\theta\cos\phi$
4. flight path angle, $\sin\gamma^*+\cos\theta\left(\cos\beta\cos\phi\sin\alpha+\sin\beta\sin\phi\right)-\cos\alpha\cos\beta\sin\theta=0$

We generally view the set of trim viable trim points, $\mathcal{T}$, in the state-control-parameter space, $\mathcal{X}\times\mathcal{U}\times\mathrm{M}\subset R^{n+m+k}$. Typically, the set of trim conditions is a smooth k-dimensional submanifold of this $n+m+k$-dimensional manifold. It is common practice in bifurcation theory to project $\mathcal{T}$ onto the parameter space M. The result is the bifurcation picture. The folds of $\mathcal{T}$ project onto M as $k-1$-dimensional submanifolds of M. So they partition M into k-dimensional disjoint regions. Each region contains a distinct number of trim points.

If we project $\mathcal{T}$ onto the n-dimensional state space $\mathcal{X}$ the result is a k-dimensional subset (possibly quite complex) of $\mathcal{X}$ that is also partitioned into subsets by the folds of $\mathcal{T}$. Again each subset is associated with a distinct number of trim points. The significance of this is that the process identifies the possible trim states and identifies the number of trim points associated with each such state. This is important for control analysts and designers concerned with state to state transitions.

B. Example: GTM Phugoid Model

We would expect that since the unimpaired aircraft has two independent controls and only two states that every point in the envelope could be made an equilibrium point by proper choice of control. The only issue is that the controls are bounded. However, the situation is more complicated than that. In fact, in this case there is one and sometimes two admissible control pairs for which each point in the state space can be made an equilibrium point. Even so, maneuverability can be problematic. To understand the problem, first compute the values of the controls (T, δ_e) required to force an arbitrary point (V, γ) to be an equilibrium point.

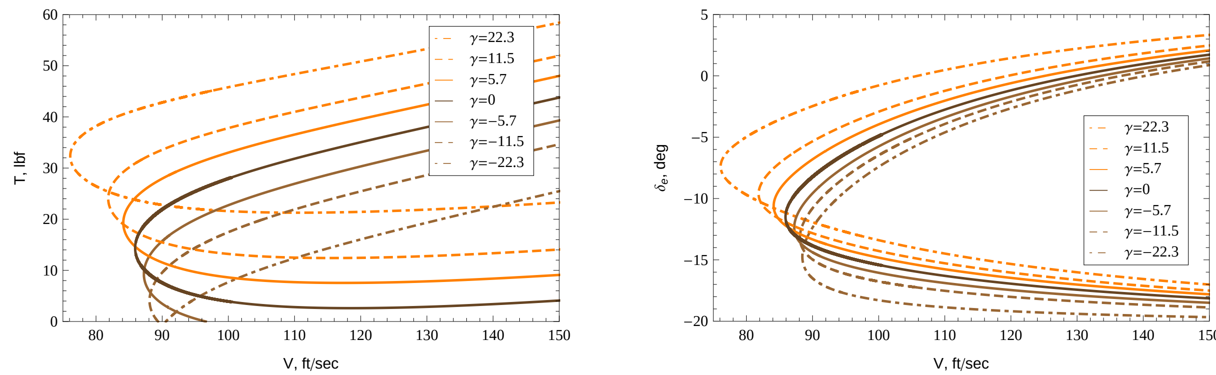

(a) Thrust (b) Elevator

Figure .3. The figure on the left shows thrust as a function of V for various values of γ. The curve on the right shows the corresponding values of elevator position. The lower branch of the thrust curves correspond to the upper branch of the elevator curves.

The results of these computations are shown in Figure .3. Each curve shows thrust or elevator position as a function of speed, V, for fixed flight path angle, γ. Each curve has two branches that meet at the bifurcation point corresponding to the stall point. As before in Figure .1, the lower thrust branch corresponds to the upper elevator branch and these trim points correspond to normal flight.

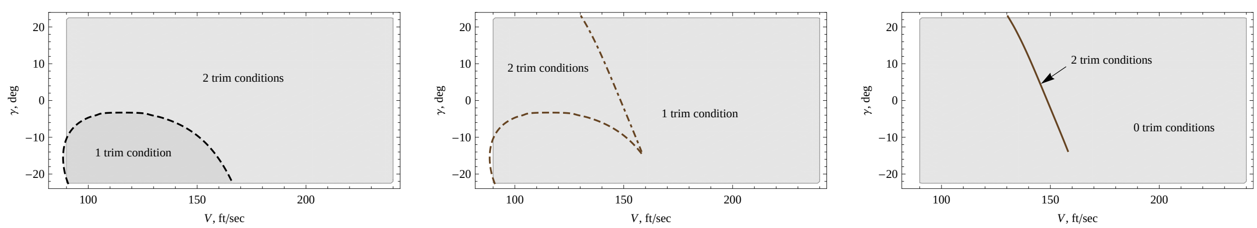

(a) Unimpaired (b) Restricted Elevator (c) Jammed Elevator

Figure .4. Each state (V, γ) in the flight envelope can be made an equilibrium point by proper selection of control pairs (T, δ_e). However, at some states, there are two admissible trim conditions and at others only one or none at all.

Notice in Figure .3 that most of the curves indicate that there are two trim conditions – one normal and one high angle of attack – for which thrust, T, and elevator position, δ_e are within their bounds. However, some descending flight path angles require require negative thrust at lower velocities in order to achieve the normal trim. So these are not valid equilibria. The situation is summarized in Figure .4 – the unimpaired case. The difficulty is that in the region admitting two trim conditions normal flight is achievable but in the region admitting one, only the high angle of attack trim is possible. Transition from normal to high angle of attack trim (or vis-versa) is difficult because of the elevator reversal. The pilot (or auto-pilot) needs to recognize the need to change control strategy accordingly. Of course, this picture is altered in significant ways if flaps, spoilers even landing gear are deployed.

In the restricted elevator case shown in Figure .4 the elevator range of motion is limited in the positive direction to 3 degrees. This severely limits the region of normal flight trim which is possible only in the area identified as having two trim conditions. Once again transition to flight out of this region requires a change to high angle of attack trim, which involves a significant increase in throttle, a decrease in elevator and results in a reversal in the effect of elevator.

V. Conclusions

In this paper we continue an examination of mechanisms of LOC. The main focus here is on the impact of control constraints, including those induced by actuator impairment, on the maneuverability within the admissible flight envelope. We used the phugoid dynamics of the GTM to provide a simple illustration of safe set computation and the effect of failures on the safe set. We examined maneuverability by identifying steady motions within the safe set and illustrated how the set of trim points can change structure when actuator impairment occurs.

An aircraft is trimmed to achieve a desired steady motion such as straight and level flight or a coordinated turn. The specification expressed as a set of algebraic equations is called the *trim condition.* The specification is generally made in terms of a set of k parameters. For example, in the case of straight and level flight we might consider speed and flight path angle to be parameters ($k = 2$). In the case of a coordinated turn we might consider, speed, flight path angle and angular velocity (equivalently, turn radius), so $k = 3$. To achieve the specified trim we need to identify the required controls and the associated state. These are obtained as solutions to the *trim equations.* For each trim condition and fixed parameters there may be zero, one, or more corresponding pairs of control and state values. We call these the *trim points* corresponding to the trim condition. For a trim point to be viable, the control must be within the allowable control set and the state must be within the safe set. The trim condition is viable only if it is associated with at least one viable trim point.

The trim equations depend on the values specified for the k trim parameters. This is a classic static bifurcation problem. Typically, the solution set is a smooth k-dimensional submanifold of an $n + m + k$-dimensional space of states, controls and parameters. The solution manifold is divided into components by co-dimension one bifurcation sets. In general, we can associate each trim point with a specific component of the solution manifold. In the phugoid example, the two dimensional solution set has two components. We identified these as *normal* and *high angle of attack.* Not all of these are viable.

We considered transitions between trim points and showed that transition from one trim condition could require moving from one trim point to another which belongs to a different component. In this case, the control properties at the two trim conditions would be quite different, thereby requiring a change in strategy for regulating around the new trim condition.

References

[1] Russell, P. and Pardee, J., "Final Report: JSAT Loss of Control: Results and Analysis," Tech. rep., Federal Aviation Administration: Commercial Airline Safety Team, 2000.

[2] Ranter, H., "Airliner Accident Statistics 2006," Tech. rep., Aviation Safety Network, 2007.

[3] Anonymous, "Statistical Summary of Commercial Jet Airplane Accidents - Worldwide Operations 1959-2007," Tech. rep., Boeing Corporation, 2008.

[4] Lambregts, A. A., Nesemeier, G., Wilborn, J. E., and Newman, R. E., "Airplane Upsets: Old Problem, New Issues," *AIAA Modeling and Simulation Technologies Conference and Exhibit*, AIAA, Honolulu, Hawaii, 2008.

[5] Wilborn, J. E. and Foster, J. V., "Defining Commercial Aircraft Loss-of-Control: a Quantitative Approach," *AIAA Atmospheric Flight mechanics Conference and Exhibit*, AIAA, Providence, Rhode Island, 16-19 August 2004.

[6] Kwatny, H. G., Bennett, W. H., and Berg, J. M., "Regulation of Relaxed Stability Aircraft," *IEEE Transactions on Automatic Control*, Vol. AC-36, No. 11, 1991, pp. 1325–1323.

[7] Kwatny, H. G., Dongmo, J.-E. T., Chang, B. C., Bajpai, G., Yasar, M., and Belcastro, C., "Aircraft Accident Prevention: Loss-of-Control Analysis," *AIAA Guidance, Navigation and Control Conference*, Chicago, 10-13 August 2009.

[8] Lygeros, J., "On Reachability and Minimum Cost Optimal Control," *Automatica*, Vol. 40, 2004, pp. 917–927.

[9] Oishi, M., Mitchell, I. M., Tomlin, C., and Saint-Pierre, P., "Computing Viable Sets and Reachable Sets to Design Feedback Linearizing Control Laws Under Saturation," *45th IEEE Conference on Decision and Control*, IEEE, San Diego, 2006, pp. 3801–3807.

[10] Feuer, A. and Heymann, M., "Ω-Invariance in Control Systems wiyh Bounded Controls," *Journal of mathematical Analysis and Applications*, Vol. 53, 1976, pp. 26–276.

[11] Jordan, T., Langford, W., Belcastro, C., Foster, J., Shah, G., Howland, G., and Kidd, R., "Development of a Dynamically Scaled Generic Transport Model Testbed for Flight Research Experiments," *AUVSI Unmanned Unlimited*, Arlington, VA, 2004.

[12] Kwatny, H. G. and Blankenship, G. L., *Nonlinear Control and Analytical Mechanics: a computational approach*, Control Engineering, Birkhauser, Boston, 2000.

[13] Murch, A. M. and Foster, J. V., "Recent NASA Research on Aerodynamic Modeling of Post-Stall and Spin Dynamics of Large Transport Aircraft," 8-11 January 2007.

[14] Morelli, E. A., "Global Nonlinear Aerodynamic Modeling Using Multivariate Orthogonal Functions," *Journal of Aircraft*, Vol. 32, No. 2, 1995, pp. 270–277.

[15] Morelli, E. A. and DeLoach, R., "Wind Tunnel Database Development using Modern Experiment Design and Multivariate Orthogonal Functions," *41st AIAA Aerospace Sciences Meeting and Exhibit*, AIAA Paper 2003-0653, Reno, NV, January 2003.

[16] Lanchester, F. W., *Aerodonetics*, Constable and Company, London, 1908.

[17] Anonymous, "Aircraft Accident Report – United Airlines Flight 232," Tech. Rep. NTSB/AAR-90/06, National Transportation Safety Board, 1990.

[18] Lygeros, J., Tomlin, C., and Sastry, S., "Controllers for reachability specifications for hybrid systems," *Automatica*, Vol. 35, No. 3, 1999, pp. 349–370.

[19] Berg, J. and Kwatny, H. G., "An Upper Bound on the Structurally Stable Regulation of a Parameterized Family of Nonlinear Control Systems," *Systems and Control Letters*, Vol. 23, 1994, pp. 85–95.

[20] Berg, J. and Kwatny, H. G., "A Canonical Parameterization of the Kronecker Form of a Matrix Pencil," *Automatica*, Vol. 31, No. 5, 1995, pp. 669–680.

[21] Berg, J. M. and Kwatny, H. G., "Unfolding the Zero Structure of a Linear Control System," *Linear Algebra and its Applications*, Vol. 235, 1997, pp. 19–39.

[22] Wonham, W. M., *Linear Multivariable Control: A Geometric Approach*, Springer-Verlag, NY, 3rd ed., 1985.

[23] Tomlin, C., Lygeros, J., and Sastry, S., "Aerodynamic Envelope Protection using Hybrid Control," *American Control Conference*, Philadelphia, 1998, pp. 1793–1796.

[24] Unnikrishnan, S. and Prasad, J. V. R., "Carefree Handling Using Reactionary Envelope Protection Method," *AIAA Guidance, Navigation and Control Conference and Exhibit*, Keystone, CO, 21-24 August 2006.

[25] Well, K. H., "Aircraft Control Laws for Envelope Protection," *AIAA Guidance, Navigation and Control Conference*, Keystone, Colorado, 21-24 August 2006.

[26] Glover, J. D. and Schweppe, F. C., "Control of Linear Systems with Set Constrained Disturbances," *IEEE Transactions on Automatic Control*, Vol. 16, No. 5, 1971, pp. 411–423.

[27] Blanchini, F., "Feedback Control for Linear Time-Invariant Systems with State and Control Bounds in the Presence of Uncertainty," *IEEE Transactions on Automatic Control*, Vol. 35, No. 11, 1990, pp. 1231 – 1234.

[28] Bitsoris, G. and Gravalou, E., "Comparison Principle, Positive Invariance and constrained regulation of Nonlinear Systems," *Automatica*, Vol. 31, No. 2, 1995, pp. 217–222.

[29] Bitsoris, G. and Vassilaki, M., "Constrained Regulation of Linear Systems," *Automatica*, Vol. 31, No. 2, 1995, pp. 223–227.

[30] ten Dam, A. A. and Nieuwenhuis, J. W., "A Linear programming Algorithm for Invariant Polyhedral Sets of Discrete-Time Linear Systems," *Systems and control Letters*, Vol. 25, 1995, pp. 337–341.

[31] Sethian, J. A., "Evolution, Implementation, and Application of Level Set and Fast Marching Methods for Advancing Fronts," *Journal of Computational Physics*, Vol. 169, 2001, pp. 503–555.

[32] Thomas, S., Kwatny, H. G., and Chang, B. C., "Nonlinear Reconfiguration for Asymmetric Failures in a Six Degree-of-Freedom F-16," *American Control Conference*, IEEE, Boston, MA, June/July 2004, pp. 1823–1829.

[33] Thomas, S., Kwatny, H. G., and Chang, B. C., "Bifurcation Analysis of Flight Control Systems," *IFAC World Congress*, Prague, 2005.

[34] Goman, M. G., Khramtsovsky, A. V., and Kolesnikov, E. N., "Evaluation of Aircraft Performance and Maneuverability by Computation of Attaiable Equilibrium Sets," *Journal of Guidance, Control and Dynamics*, Vol. 31, No. 2, 2008, pp. 329–339.

[35] Thomas, S., *Reconfiguration and bifurcation in flight controls*, Ph.D. thesis, Drexel University, Philadelphia, December 2004. [Online] http://dspace.library.drexel.edu/handle/1860/385.

[36] Bajpai, G., Beytin, A., Thomas, S., Yasar, M., Kwatny, H. G., and Chang, B. C., "Nonlinear Modeling and Analysis Software for Control Upset Prevention and Recovery of Aircraft," *AIAA Guidance, Navigation and Control Conference*, AIAA, Honolulu, Hawaii, 18-21 August 2008.